Verification of Link Performance Prediction for CDMA

Michał Panek and Przemysław Czerepiński
Nokia Siemens Networks, Research, Radio Systems, Wrocław, Poland
michal.panek@nsn.com

Abstract—**Link performance prediction is widely used in system level simulations. For CDMA, link prediction formulas have been reported, however, in contrast to OFDM, the verification step has not been well documented. The goal of this paper is, therefore, to perform the verification step of the link performance prediction model for the CDMA radio interface. The analysis was performed by simulating the physical layer TX and RX chain in the context of the WCDMA HSDPA standard. Based on comprehensive simulation results, the correctness of the CDMA link prediction model is confirmed for single stream as well as MIMO transmission with the rake and LMMSE receivers. Thus, analytical abstraction of the physical layer can be employed with confidence at system level simulation.**

Index Terms—link prediction, link to system interface, effective SINR, post-receiver SINR, CDMA

I. INTRODUCTION

A link-to-system interface lies at the heart of modern wireless communication system modelling. It allows compressing a large number of radio link conditions, such as the channel state, interference, antenna configuration, radio interface technology, physical resource allocation etc. into a single "effective" or "post-receiver" SINR value. Thus, the receiver performance can be accurately predicted without the need of extensive link simulations covering the entire parameter space.

Recent years saw significant interest in SINR calculation for OFDM; in particular, MIESM (mutual information effective SINR mapping) and EESM (exponential effective SINR mapping) [1][2] were demonstrated accurately to predict link performance. For CDMA, post-receiver SINR or MSE formulas were given by a number of authors [3][4][5][6][9], with the assumption of a linear receiver.

To ensure accurate system modelling, it is essential that the accuracy of SINR prediction be verified. In the case of MIESM and EESM, comprehensive verification results are available in [1][7][8] as well as other sources. It is therefore surprising that such results do not seem to have been published for CDMA. We identified two references: Szabo *et al*. provide verification results in terms of the raw bit error rate (BER) [9], which does not include the impact of a number of physical layer processing units, e.g. interleaving or error correction. Wrulich and Rupp provide one verification result for the HSDPA TX-RX chain in the case of single stream transmission [6].

The motivation for this paper is to provide a set of simulation results, verifying CDMA link prediction formulas. It should be noted that we use the term CDMA in a standard-agnostic manner i.e. covering any direct-sequence code division multiple access radio interface technology. However, for the sake of verification, we focus on a specific, representative instance of CDMA, namely the WCDMA FDD HSDPA (wideband CDMA, frequency division duplexing, high speed downlink packet access) standard.

In the first part of this paper, we recall the analytical post-receiver SINR formulation, based on [3][4][5][6][9]. The goal of the analytical formulation is to transform the set of simulation conditions, including the TX signal and interference power, propagation channel state, antenna configuration etc. into a single, AWGN-equivalent SISO SINR value. In the second part of the paper, we compare the analytically obtained BLER vs. SINR prediction to actual AWGN link level performance. Analytical link prediction is demonstrated to be very accurate for both the single stream and MIMO transmission under the chosen simulation assumptions. Further, we discuss the limits of the analytical model as well as the needed extensions to cope with e.g. a high Doppler frequency scenario.

The remainder of this paper is structured as follows: Section II describes the role of the link-to-system interface and the verification methodology. Section III provides the signal model description, and the SINR formulas are given in Section IV. Simulation results are provided in Section V and conclusion is drawn in Section VI.

II. LINK-TO-SYSTEM INTERFACE

A. Link Performance Prediction in System Simulations

Wireless system modelling is typically performed at two stages, called *link* level (LL) and *system* level (SL). A SL simulation comprises a number of radio links. In principle, a separate LL simulation could be performed for each link. However, the complexity of such modelling can be prohibitive. Instead, as illustrated in figure 1, an abstraction of link performance is utilized that maps the *instantaneous* link conditions into an AWGN-equivalent SINR value, which can be referenced to AWGN link performance in order to obtain an estimate of the block error rate (BLER).

Conceptually, the post-receiver SINR corresponds to the SINR at the output of the receiver's chip processor or equalizer. Thus, the LL-SL interface consists of two parts:

- An abstraction of the chip equalizer.
- A set of BLER vs. SINR curves for the relevant

978-1-4673-0990-5/12/$31.00 ©2012 IEEE

modulation and coding formats in AWGN.

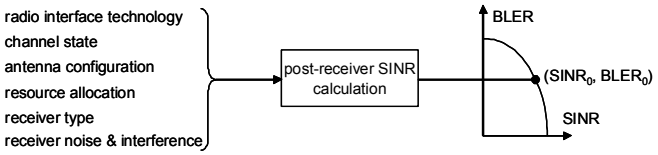

Figure 1 – LL-SL interface principle.

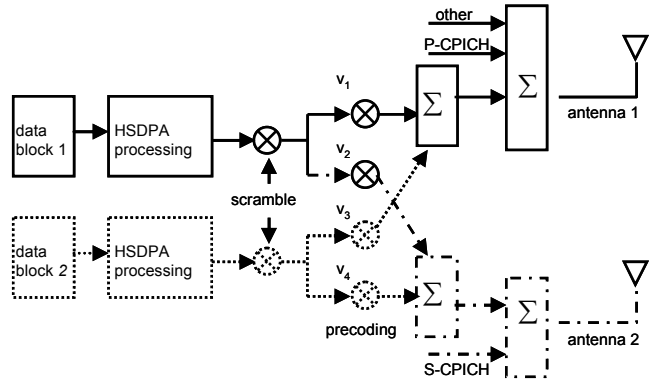

Figure 2 – Generic transmitter structure

B. Link-to-System Interface Verification Methodology

In order to confirm the correctness of the LL-SL interface, the HSDPA physical layer TX-RX chain was implemented, including turbo coding, rate matching, interleaving, QAM, spreading and scrambling. Propagation effects were modelled by means of the WSS-US (wide sense stationary, uncorrelated scattering) model, using the Pedestrian A, Vehicular A and Typical Urban power delay profiles (Table 1).

Post-receiver SINR was calculated analytically and classified into narrow bins of approximately 0.2 dB. For each received data block, the SINR bin and the CRC pass or fail decision was recorded. With a sufficiently long simulation, the BLER vs. effective SINR performance curve was constructed and compared to the reference performance of the symbol processing chain alone (effectively, the turbo codec and QAM mapper) under AWGN.

III. SIGNAL MODEL DESCRIPTION

Figure 2 presents the generic transmitter structure for HSDPA. Up to two data blocks can be transmitted concurrently to achieve spatial multiplexing. Each block undergoes HSDPA-compliant processing according to [10]-[13]. The resulting chip sequences can be precoded by the weights v_i and transmitted from up to two antennas. Other channels, such as primary and secondary pilot or other broadcast channels are also present on antennas 1 or 2.

A number of transmission modes can be configured:

- Single stream, single antenna transmission. The weight v_1 is set to 1 and the remaining weights to 0. The dotted and dashed-dotted parts of the diagram are inactive.
- Single stream, dual antenna transmission (TxAA). The weights v_1 and v_2 have non-zero values according to [13]. The weights v_3 and v_4 are set to 0 and the dotted part of the diagram is inactive.
- Dual stream, dual antenna transmission (D-TxAA). All weights v_i have non-zero values according to [13]. All parts of the diagram are active.

The transmitted chip sequence, $\mathbf{s}(m)$, at baseband is a complex-valued multiplex of OVSF (Orthogonal Variable Spreading Factor) code-spread sub-signals, scrambled by a base station specific long code and constructed in line with standard rules. $\mathbf{s}(m)$ is a vector sized $N_t(F+L)\times 1$:

$$\boldsymbol{s}(m) = [s_1(m+F-D-1), s_2(m+F-D-1), \dots s_{N_t}(m+F-D-1), \dots, s_{N_t}(m-D-L)]^T$$

where N_t is the number of Tx antennas, F the length of the linear receive filter, L the channel delay spread expressed in chip periods and D, $0 \le D < F$, a receiver delay parameter.

It is assumed in the following that the channel 'taps' coincide with the signal chip timing and the pulse shaping is absent. The received chip sequence $\mathbf{r}(m)$, sized $N_rF\times 1$ (N_r is the number of Rx antennas), can be written as:

$$\boldsymbol{r}(m) = \boldsymbol{H}^T \boldsymbol{s}(m) + \boldsymbol{n}(m)$$

where $\mathbf{n}(m)$, sized $N_rF\times 1$, is the receiver noise and interference vector and $\mathbf{H}^T$, $N_rF\times N_t(F+L)$, is the channel coefficient matrix:

$$\boldsymbol{H}^T = \begin{bmatrix} \boldsymbol{h} & \boldsymbol{0}_{N_r,N_t} & \boldsymbol{0}_{N_r,N_t} & \cdots & \boldsymbol{0}_{N_r,N_t} \\ \boldsymbol{0}_{N_r,N_t} & \boldsymbol{h} & \boldsymbol{0}_{N_r,N_t} & & \boldsymbol{0}_{N_r,N_t} \\ & \vdots & & \ddots & \vdots \\ \boldsymbol{0}_{N_r,N_t} & \boldsymbol{0}_{N_r,N_t} & \boldsymbol{0}_{N_r,N_t} & \cdots & \boldsymbol{h} \end{bmatrix}$$

$\mathbf{H}$ is a convolution matrix of the channel impulse response, $\mathbf{h}$, sized $N_r\times N_t(L+1)$:

$$h = \begin{bmatrix} h_{1,1}(1) & h_{1,2}(1) & \cdots & h_{1,N_t}(1) \\ h_{2,1}(1) & h_{2,2}(1) & & \vdots \\ \vdots & & \ddots & \vdots \\ h_{N_r,1}(1) & h_{N_r,2}(1) & \cdots & h_{N_r,N_t}(1) \end{bmatrix}$$

It may happen that some channels undergo precoding (beamforming) and others do not. In such scenarios, the equivalent channel matrix $\mathbf{\Gamma}^T$, $N_rF\times N_s(F+L)$, is relevant [6], representing the channel after precoding weights are applied:

$$\boldsymbol{\Gamma}^T = \begin{bmatrix} \boldsymbol{h_e} & \boldsymbol{0}_{N_r,N_s} & \boldsymbol{0}_{N_r,N_s} & \cdots & \boldsymbol{0}_{N_r,N_s} \\ \boldsymbol{0}_{N_r,N_s} & \boldsymbol{h_e} & \boldsymbol{0}_{N_r,N_s} & & \boldsymbol{0}_{N_r,N_s} \\ & \vdots & & \ddots & \vdots \\ \boldsymbol{0}_{N_r,N_s} & \boldsymbol{0}_{N_r,N_s} & \boldsymbol{0}_{N_r,N_s} & \cdots & \boldsymbol{h_e} \end{bmatrix}$$

where N_s is the number of transmitted data streams,

$$\boldsymbol{h_e} = \boldsymbol{h}(\boldsymbol{I_{L+1}} \otimes \boldsymbol{B})$$

is an equivalent beamformed channel (MIMO channel) impulse response. $\mathbf{B}$ is an $N_t\times N_s$ matrix containing precoding weights, $\mathbf{I}_{L+1}$ is an identity matrix sized $L+1$ and $\otimes$ denotes the Kronecker product.

The linear receiver estimates the transmitted chip sequence as:

$$\tilde{\boldsymbol{s}}(\boldsymbol{m}) = \boldsymbol{W}^{\boldsymbol{T}}\boldsymbol{r}(\boldsymbol{m})$$

where $\mathbf{W}^T$ is the receiver filter sized $N_s \times N_r F$. $\tilde{\mathbf{s}}(m)$ is sized $N_s \times 1$.

IV. SINR CALCULATION

A. General Formula

In this Section, we recall the SINR formulas for linear CDMA receivers as reported by a number of authors in the case of SISO [3][4][5] and MIMO [6][9]. The formulation is generic so that it covers all HSDPA transmission modes covered in Section III.

Post-receiver SINR, calculated per one physical channel (i.e. one OVSF code) and one QAM symbol of the *i*-th data stream is given by:

$$SINR_{S,i} = \frac{P_{S,i}}{I_{p,i}+I_{np,i}+(N_S-1)I_{IS,i}+N_i} \quad (1)$$

where $P_{S,i}$ is the "per QAM symbol" post-receiver signal power, $I_{p,i}$ is the self-interference term originating from *i*-th stream, $I_{np,i}$ is the self-interference term originating from non-precoded channels, $I_{IS,i}$ is the inter-stream interference term and N_i is the receiver noise and other cell interference term.

$P_{S,i}$ can be written as:

$$P_{S,i} = \frac{SF}{N_C}\frac{E_{C,Data}}{I_{or}}\frac{\hat{I}_{or}}{N_S}|\boldsymbol{w}_i^T\boldsymbol{\Gamma}_i^T\boldsymbol{\delta}|^2$$

where SF is the spreading factor and N_C is the number of channels used to transmit the data block. $E_{c,Data}/I_{or}$ is the transmit power fraction allocated to the data channels, $\mathbf{w}_i$ is the *i*-th row of $\mathbf{W}$, representing the receive filter of the *i*-th data stream. $\boldsymbol{\delta}$ is a delay vector that extracts the rows of the channel matrix at the receive filter's delay. Both $\mathbf{w}$ and $\boldsymbol{\delta}$ depend on the receiver type as explained in the following. $\hat{I}_{or}$ denotes the total received carrier power. $\boldsymbol{\Gamma}_i$ is the *i*-th stream's equivalent channel matrix.

The *i*-th stream's self-interference term $I_{p,i}$ can be written as:

$$I_{p,i} = \frac{E_{C,Data}}{I_{or}}\frac{\hat{I}_{or}}{N_S}(\boldsymbol{w}_i^T\boldsymbol{\Gamma}_i^T\widehat{\boldsymbol{\delta}}\widehat{\boldsymbol{\delta}}^{\boldsymbol{T}}\boldsymbol{\Gamma}_i^*\boldsymbol{w}_i^*)$$

where $\widehat{\boldsymbol{\delta}} = diag(\mathbf{1}-\boldsymbol{\delta})$.

The term $I_{np,i}$ can be written as:

$$I_{np,i} = \sum_{iTx=1}^{N_t}\frac{E_{C,nb,iTx}}{I_{or}}\hat{I}_{or}(\boldsymbol{w}_i^T\boldsymbol{\Gamma}_{iTx}^T\widehat{\boldsymbol{\delta}}\widehat{\boldsymbol{\delta}}^{\boldsymbol{T}}\boldsymbol{\Gamma}_{iTx}^*\boldsymbol{w}_i^*)$$

where iTx is the Tx antenna index, $E_{c,nb,iTx}/I_{or}$ is the transmit power fraction allocated to the non-precoded channels on the iTx-th antenna. $\mathbf{H}_{iTx}$ is the part of $\mathbf{H}$ containing the channel coefficients between iTx-th antenna and the receiver. In the case of 2 Tx antennas, $\mathbf{H_1}$ is formed from odd columns and $\mathbf{H_2}$ from even columns of $\mathbf{H}$.

In the case of spatial multiplexing, the base station transmits multiple data streams on the same physical resources, leading to inter-stream interference $I_{IS,i}$:

$$I_{IS,i} = \frac{E_{C,Data}}{I_{or}}\frac{\hat{I}_{or}}{N_S}(\frac{SF}{N_C}\boldsymbol{w}_i^T\boldsymbol{\Gamma}_j^T\boldsymbol{\delta}\boldsymbol{\delta}^{\boldsymbol{T}}\boldsymbol{\Gamma}_j^*\boldsymbol{w}_i^* + (\boldsymbol{w}_i^T\boldsymbol{\Gamma}_j^T\widehat{\boldsymbol{\delta}}\widehat{\boldsymbol{\delta}}^{\boldsymbol{T}}\boldsymbol{\Gamma}_j^*\boldsymbol{w}_i^*) \quad (2)$$

where j is the index of the other stream, in the case of dual stream transmission. The first term in parenthesis in (2) corresponds to the interference originating from the same OVSF code on the other stream and at the same channel tap. The second term in the parenthesis is interference originating from all OVSF codes on the other stream and at other channel taps.

Assuming white intercell interference, the noise and interference term N_i can be written as:

$N_i = \boldsymbol{w}_i^T\boldsymbol{C}_W\boldsymbol{w}_i^*$

where

$$\boldsymbol{C}_W = \begin{bmatrix} \sigma_1^2 & 0 & 0 & & 0 \\ 0 & \sigma_2^2 & 0 & \cdots & 0 \\ 0 & 0 & \sigma_1^2 & & 0 \\ & \vdots & & \ddots & \vdots \\ 0 & 0 & 0 & \cdots & \sigma_2^2 \end{bmatrix}$$

and σ_{iRx}^2 is noise and intercell interference power seen at the iRx-th receive antenna.

B. Receivers

1) Rake receiver

The rake receiver filter is given by $\boldsymbol{W} = \boldsymbol{H}^H\boldsymbol{\delta}$, where $\boldsymbol{\delta}$ is:

$$\boldsymbol{\delta} = \left[\underbrace{0\ \cdots\ 0}_{L}\ 1\ 0\ \cdots 0\right]^T$$

2) LMMSE receiver

In the case of the LMMSE (Linear Minimum Mean Square Error) receiver, in principle there is room for optimizing the delay parameter $\boldsymbol{\delta}$, although this is likely to be problematic in a practical implementation. In this paper, it is assumed that the delay is by default set to:

$$\boldsymbol{\delta} = \left[\underbrace{0\ \cdots\ 0}_{\lfloor(F+L)/2\rfloor}\ 1\ 0\ \cdots 0\right]^T \quad (3)$$

The LMMSE receiver filter is given by:

$$\boldsymbol{W}^T = \boldsymbol{\delta}_{\boldsymbol{M}}\boldsymbol{H}^*(\boldsymbol{H}^{\boldsymbol{T}}\boldsymbol{H}^* + \boldsymbol{C}_{\boldsymbol{W}})^{-\mathbf{1}} \quad (4)$$

where

$$\boldsymbol{\delta}_{\boldsymbol{M}}^{\boldsymbol{T}} = \left[\mathbf{0}_{N_S,N_S\lfloor(F+L)/2\rfloor}, \boldsymbol{I}_{N_S}, \mathbf{0}_{N_S,N_S(\lfloor(F+L)/2\rfloor-1)}\right]^T$$

is the combined delay for N_s data streams. In the case of MIMO transmission, $\mathbf{H}$ should be replaced with $\boldsymbol{\Gamma}$ in (4).

V. VERIFICATION RESULTS

The above post-receiver SINR equations were verified using an HSDPA link level simulator, in line with the methodology of Section II.B. The simulation assumptions have been collected in Table 1. The following figures

contain three groups of plots, corresponding to QPSK, 16QAM and 64QAM. For all verification scenarios, the reference AWGN curve was obtained for the SISO case so that the long-term average and instantaneous SINRs are equal. The remaining curves show BLER vs. instantaneous SINR, calculated using eq. (1) in the presence of multipath time-varying channel profiles. The SINR is calculated at every time slot i.e. 3 times per the 2ms interleaving depth and then averaged. This is justified due to the low terminal speed of 3km/h and the 2GHz carrier frequency.

If the theoretical SINR calculation formulas are correct, the curves corresponding to the AWGN reference as well as the multipath profiles should be well matched. Due to limited space, a representative subset of the available verification results is shown.

A. Single Antenna Transmission

Figures 3 and 4 show verification results for the single antenna rake and dual antenna LMMSE receiver case. $E_{c,Data}/I_{or}$ was set to 0.7 and the remaining TX power was allocated to common channels. An excellent match is observed between the reference and test cases. In some cases the 64QAM verification is missing for the Typical Urban channel; this is because the required SINR range cannot be reached due to high self-interference.

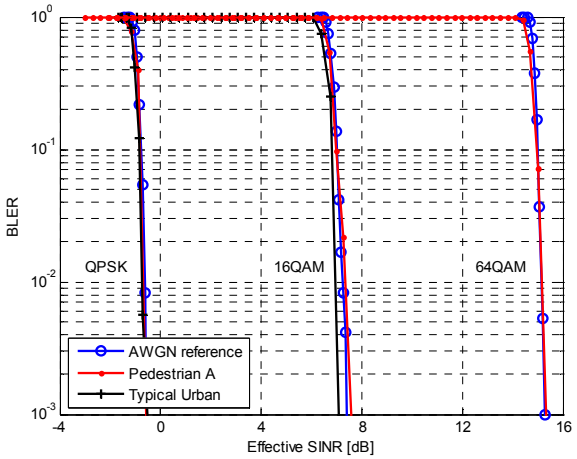

Figure 3 – Verification results for rake, SISO.

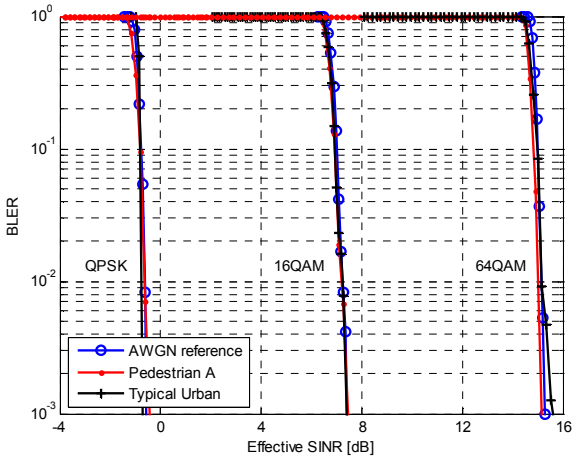

Figure 4 – Verification results for LMMSE, SIMO.

Table 1 – Simulation assumptions.

Parameter	Value
coding rate & modulation	1/3 QPSK, 1/2 16QAM, 2/3 64QAM
interleaving depth	2 ms (TTI, transmission time interval)
multipath power delay profiles	PedA: [0 0.11 0.19 0.41] us, [0 -9.7 -19.2 -22.8] dB VehA: [0 0.31 0.71 1.09 1.73 2.51] us [0 -1 -9 -10 -15 -20] dB TU: [0 0.2 0.6 1.6 2.4 5.0] us [-3 0 -2 -6 -8 -10] dB
Doppler spectrum	Jakes
terminal speed	3, 30, 60 km/h
carrier frequency	2 GHz
$E_{c,Data}/I_{or}$	0.7
code allocation	15 x SF16 codes for HSDPA data

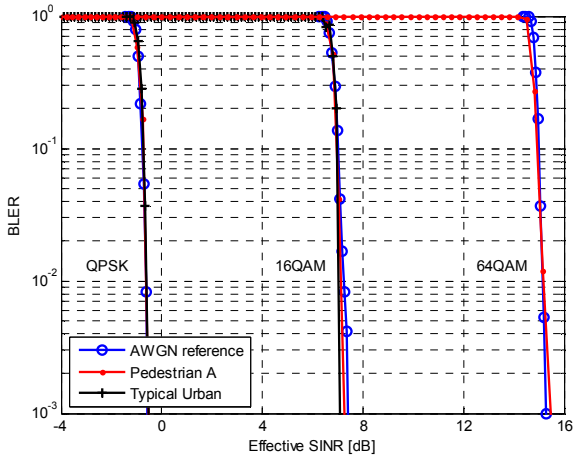

Figure 5 – Verification results for 2x2 dual stream MIMO, primary stream.

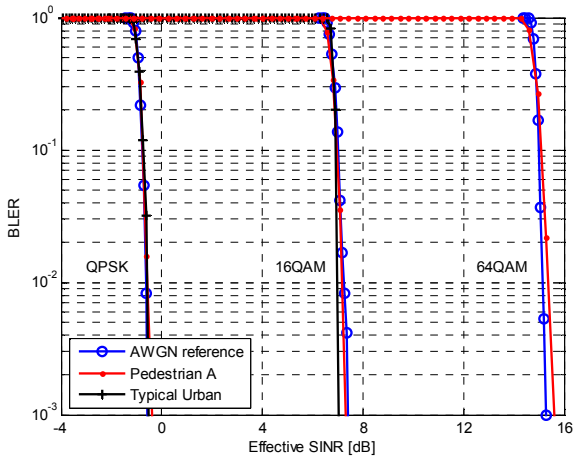

Figure 6 – Verification results for 2x2 dual stream MIMO, secondary stream.

B. Dual Antenna Transmission

Figures 5 and 6 show verification results for 2x2 dual-stream MIMO. Figure 7 verifies the scenario where the terminal is aware of the presence of single stream, single antenna transmission only. However, the network is MIMO-enabled so that a secondary pilot is transmitted from the second base station antenna to support MIMO terminals. Thus, the secondary pilot forms interference towards the non-MIMO terminal. As can be verified, the post-receiver

SINR is correctly evaluated in all cases.

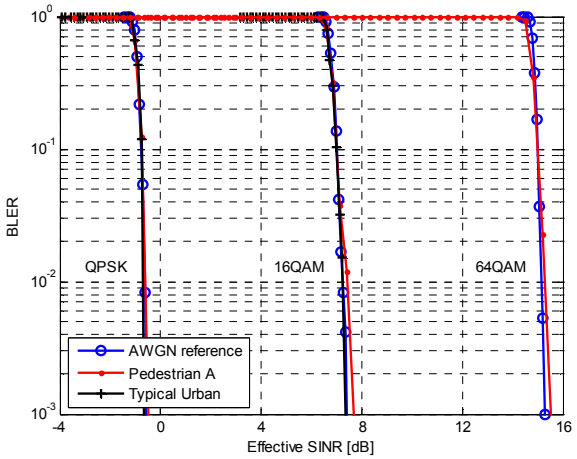

Figure 7 – Verification results for LMMSE, SIMO. Secondary pilot present on TX antenna 2.

C. *Doppler Effect Impact*

In the verification results presented so far, the normalized interleaving depth, $\alpha = f_D T_{I/L}$, was approximately equal to 0.01, where f_D is the maximum Doppler frequency and $T_{I/L}$ is the interleaving depth. Thus, the simulation was performed well within the channel's coherence time. Figure 8 illustrates the effect of increasing α to 0.11 and 0.22 (corresponding to speeds of 30 and 60 km/h at a 2GHz carrier). As expected, the precision of post-receiver SINR gradually deteriorates as the speed grows. The accuracy can be improved at the cost of increasing the post-receiver SINR sampling rate and employing MIESM-based averaging of SINR values. On the other hand, system level simulation is typically performed at low to medium speeds as precise system modelling of high speed scenarios is challenging due to the impact of feedback loop delays and handovers.

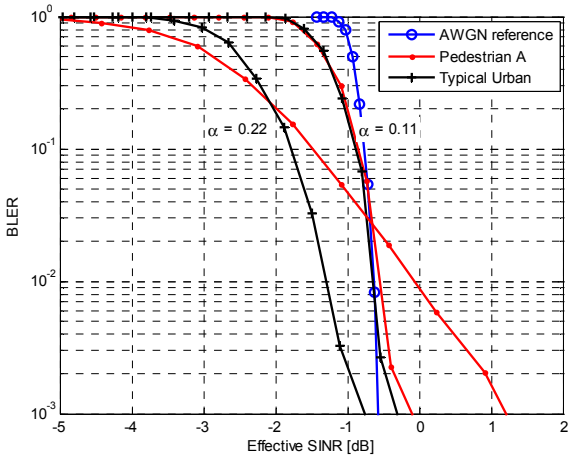

Figure 8 – Impact of the Doppler frequency, QPSK.

VI. CONCLUSION

Post-receiver SINR formulas for CDMA have been widely reported, however, the verification step has not been well documented. In this paper, after reviewing the relevant theory, the SINR formulas were validated by comprehensive HSDPA physical layer simulations. The validation covered single and dual antenna transmission, including MIMO with spatial multiplexing. Thus, the CDMA link-to-system interface, based on eq. (1), is a powerful physical layer abstraction mechanism that can be confidently employed during system simulation.

Further results were provided, illustrating the impact of the Doppler frequency on the precision of link prediction. It was found that increasing the normalized interleaving depth parameter, α, beyond 0.1 lead to significant link prediction inaccuracy; one means to improve the precision would be to employ a higher SINR sampling rate in combination with MIESM-based averaging of SINR values. In fact, such an approach could be used whenever significant SINR variations may be experienced inside the interleaving interval, due to either a high terminal speed, fast power control (not employed by HSDPA) or interference changes.

ACKNOWLEDGEMENT

We gratefully acknowledge the valuable discussion and help from Krystian Pawlak, Michał Maternia, Thomas Chapman and Wolfgang Aichmann in the course of this work.

REFERENCES

[1] Brüninghaus K., Astely D., Sälzer T., Visuri S., Alexiu A., Karger S., Seraji G. A. "Link Performance Models for System Level Simulations of Broadband Radio Access Systems", PIMRC, Berlin 2005, vol. 4, pp. 2306-2311.

[2] Tuomaala E., Haiming W. "Effective SINR approach of link to system mapping in OFDM/multi-carrier mobile network", 2nd International Conference on Mobile Technology, Applications and Systems 2005.

[3] Madhow U., Honig M. "MMSE Interference Suppression for Direct-Sequence Spread-Spectrum CDMA", IEEE Trans. on Communications, vol. 42, no. 12, pp. 3178-3188, Dec. 1994.

[4] Krauss T., Zoltowski M. "Oversampling diversity versus dual antenna diversity for chip-level equalization on CDMA downlink", 1st IEEE Sensor Array and Multichannel Signal Processing Workshop, Cambridge, MA, March 2000, pp. 47-51.

[5] Nihtila T., Kurjenniemi J., Lampinen M., Ristaniemi T. "WCDMA HSDPA Network Performance with Receive Diversity and LMMSE Chip Equalization" in IEEE 16th International Symposium on Personal, Indoor and Mobile Radio Communications 2005, pp. 1245-1249.

[6] Wrulich M., Rupp M. "Computationally Efficient MIMO HSDPA System-Level Modelling" EURASIP Journal on Wireless Communications and Networking, 2009, pp.1-14.

[7] Nasser Y., Helard J., Crussiere M. "Bit error rate prediction of coded MIMO-OFDM systems" IEEE 9th Workshop on Signal Processing Advances in Wireless Communications 2008, pp. 181-185.

[8] Wan L., Tsai S., Almgren M. "A Fading-Insensitive Performance Metric for a Unified Link Quality Model" IEEE Wireless Communications and Networking Conference 2006, vol. 4, pp. 2110-2114.

[9] Szabo A., Geng N., Seeger A., Utschick W. "Investigation on Link to System Interface for MIMO Systems" Proc. 3rd International Symposium on Image and Signal Processing and Analysis 2003, pp. 365-369.

[10] 3GPP TS 25.211 "Physical Channels and Mapping of Transport Channels onto Physical Channels (FDD)".

[11] 3GPP TS 25.212 "Multiplexing and Channel Coding (FDD)".

[12] 3GPP TS 25.213 "Spreading and Scrambling (FDD)".

[13] 3GPP TS 25.214 "Physical Layer Procedures (FDD)".